

SECTION 4

N72-29305

RADIOMETRIC IMAGES OF IR RESTSTRAHLEN

EMISSION FROM ROCK SURFACES

by

Warren A. Hovis
Laboratory for Meteorology
and Earth Sciences
Goddard Space Flight Center
Greenbelt, Md. 20771

ORIGINAL CONTAINS
COLOR ILLUSTRATIONS

INTRODUCTION

Measurements by a number of investigators, principally Lyon (1), have shown that the reststrahlen feature of silica bearing rocks, soils and unconsolidated segments, is variable with silica concentration. The maximum intensity of the reststrahlen band is found to vary from 8.8 micrometers for acidic materials rich in silica to 10.7 micrometers for ultrabasic rocks poor in silica. For remote sensing purposes the reststrahlen bands are of interest since they reduce emissivity selectively. Figure 1 shows the effect of the reststrahlen of granite, an acidic rock, and durite, an ultrabasic rock, on the emitted energy of samples at 290°K. The effect of the reststrahlen is to reduce the emitted energy and hence reduce the equivalent blackbody temperature that would be measured by a radiometer. The effect of the 9.6 micrometer ozone band, as seen from satellite measurements, is shown to illustrate why the reststrahlen of intermediate rocks cannot be sensed from a space platform. The ozone band completely masks the wavelength interval in which intermediate reststrahlen bands occur.

INSTRUMENTATION

In order to test the feasibility of remote sensing of the reststrahlen effect, a two-channel radiometer was constructed that sensed radiance in two channels simultaneously. The channels selected were 8.3 to 9.3 and 10.2 to 11.2 micrometers. The instrument had an instantaneous geometric field of view of 2° x 2° and a rotating mirror scan mechanism designed to produce contiguous scans from a DC-3 aircraft at approximately 10,000 ft. altitude. Signals were recorded on a magnetic tape recorder and subsequently converted to equivalent blackbody temperatures for both channels.

RESULTS

Measurements were made over a number of rock types in the Maryland-Pennsylvania region and samples were acquired of surface material from all areas observed. Figure 2 shows the measured emissivity of a sample of serpentine from Rockville, Md. together with the transmission of the filters used to define the two channels. Since the detectors used were thermistor bolometers there should be little spectral associated with them and it is reasonable to expect that the response functions closely follow the filter transmissions.

It can be seen in Figure 2 that the emissivity of the sample is lower in the 10.2 to 11.2 micrometer region than in the 8.3 to 9.3 micrometer region. A lower equivalent blackbody temperature would then be expected in the long wavelength channel than in the short. Figure 3 shows the measured equivalent blackbody temperatures along the aircraft nadir across the serpentine. The equivalent blackbody temperatures are in good agreement over the fields and trees bordering the exposed serpentine but differ by up to 2.5°C over the serpentine. It should be noted that reduction of particle size reduces the intensity of reststrahlen but does not shift the wavelength unless particle size is extremely small. In this case quarry dust was present on the samples and was included in the laboratory measurements shown in Figure 2.

Another area of exposed serpentine was overflowed near Cedar Hill, Pennsylvania. Figure 4 shows the measured emissivity of two samples from the area overflowed and Figure 5, the equivalent blackbody temperature observed in the nadir direction. Again the long wavelength channel shows a lower equivalent blackbody temperature than the short wavelength channel as would be expected for a low silica content rock.

A region of exposed slate was overflowed near Peach Bottom, Md. to cover an intermediate case. Figure 6 shows the laboratory measured emissivity of the slate with its reststrahlen approximately midway between the two channels. Figure 7 shows the equivalent blackbody temperatures measured along the nadir. Small temperature variations are seen; never as much as 1°C.

Beach sand is rich in silica and was used to examine the effect of acidic materials. Assateague Island, on the Eastern Shore of Maryland and Virginia, was overflowed and surface samples collected. Figure 8 shows the laboratory measured emissivity of the beach sand with a very pronounced reststrahlen feature corresponding quite closely to the short wavelength channel. Figure 9 shows the equivalent blackbody temperatures, measured at nadir, during a flight from over the Atlantic, across the island, and then over Chincoteague Bay. Over water the two

channels agree very well and show the bay water slightly warmer than the ocean. Over the island differences up to 5 and 6°C are seen with the short wavelength channel now indicating the cooler temperature. The inland or bay side of the island is marshy and more heavily vegetated than the ocean side, so the temperature differences are reduced as the sand within the instrument field of view is partially covered by water or vegetation.

The mapping ability of the instrument is shown in Figure 10. A flight was conducted parallel to the shore line of the island with the Atlantic on the left and the island on the right. Various methods of presenting a map where both a difference and the polarity of the difference could be shown were examined. The best results were obtained with a color plot where green represents little or no difference in equivalent blackbody temperature, colors tending toward red represent the case where the short wavelength channel appears cooler and colors tending toward blue represent the reverse case. Over the beach sand the color map shows the material to be rich in silica while over the ocean the green color indicates a material that is reasonably black in both channels, water. This format has been adopted for presentation of the data from the Nimbus E HRSCMR.

REFERENCE

1. Lyon, R. J. P. , Econ. Geol. 60, 715 (1965).

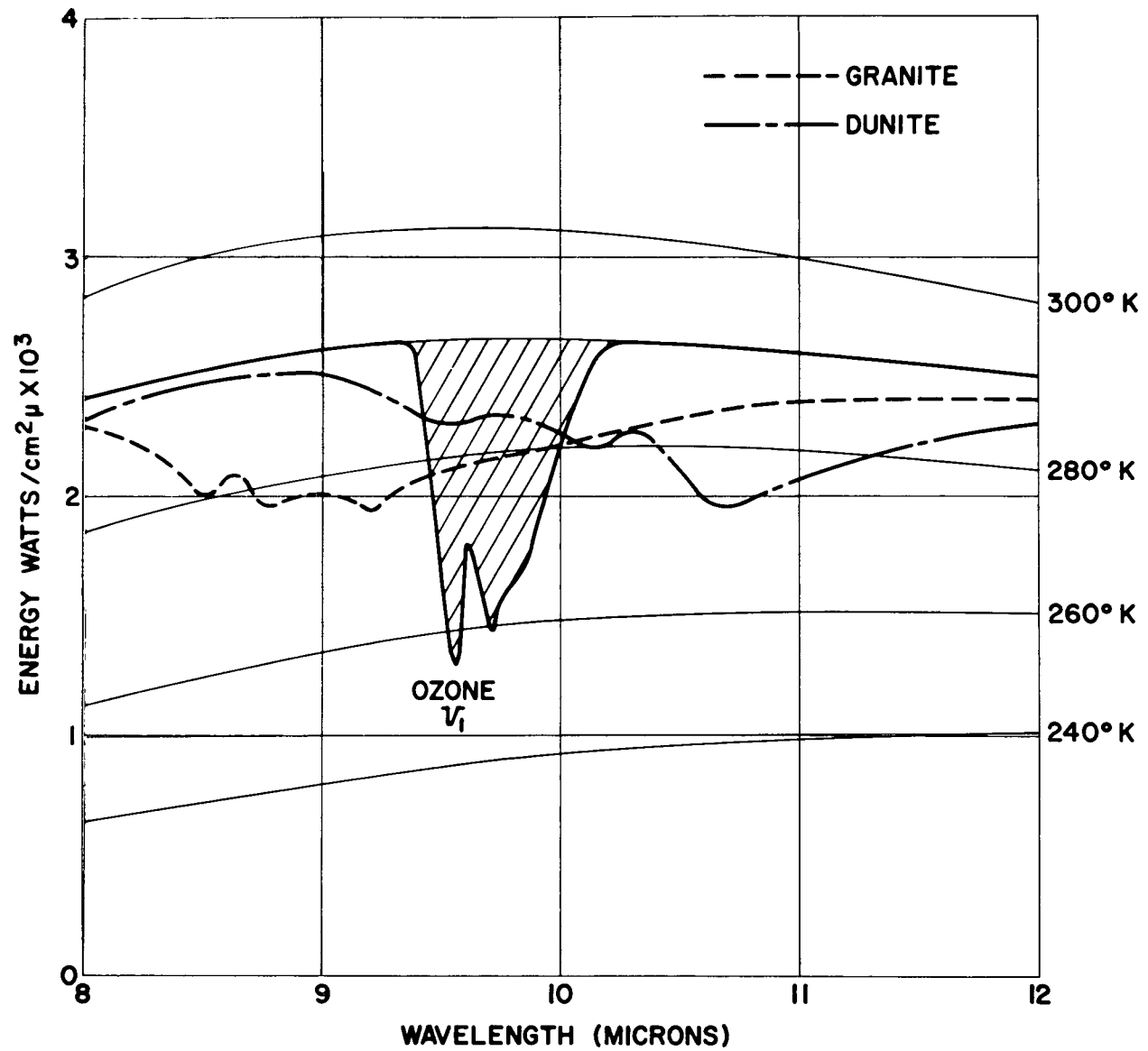


Fig. 1

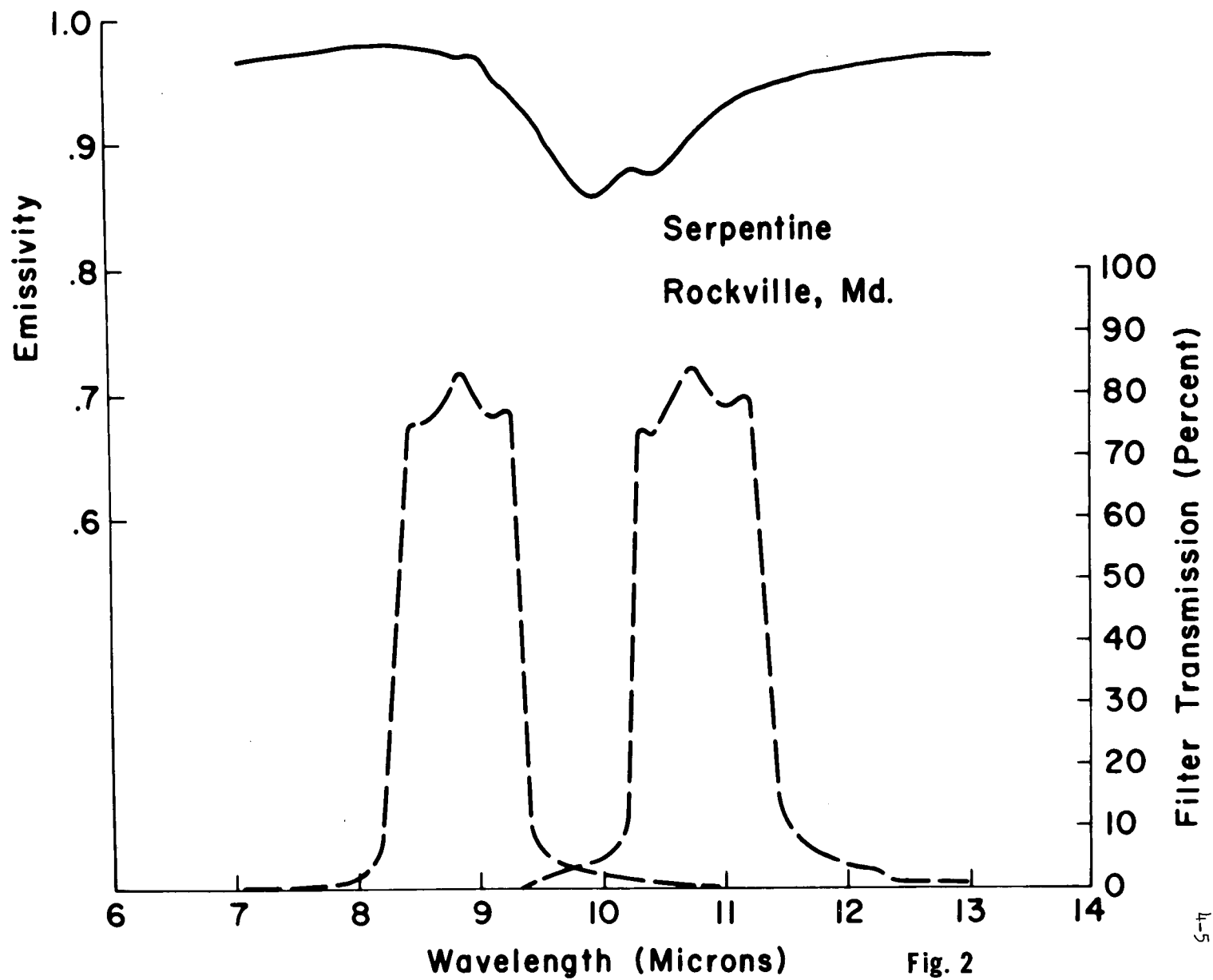


Fig. 2

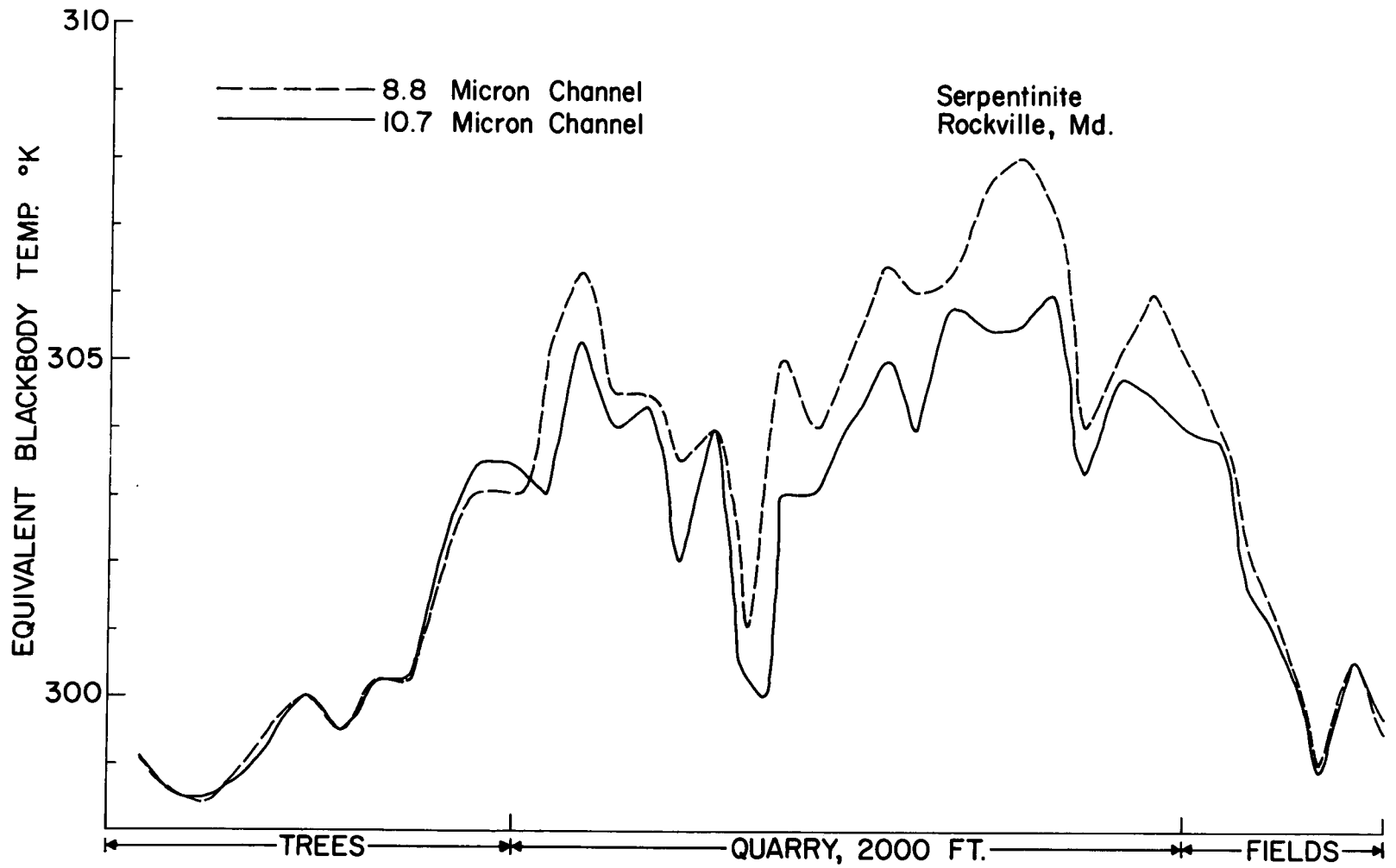


Fig. 3

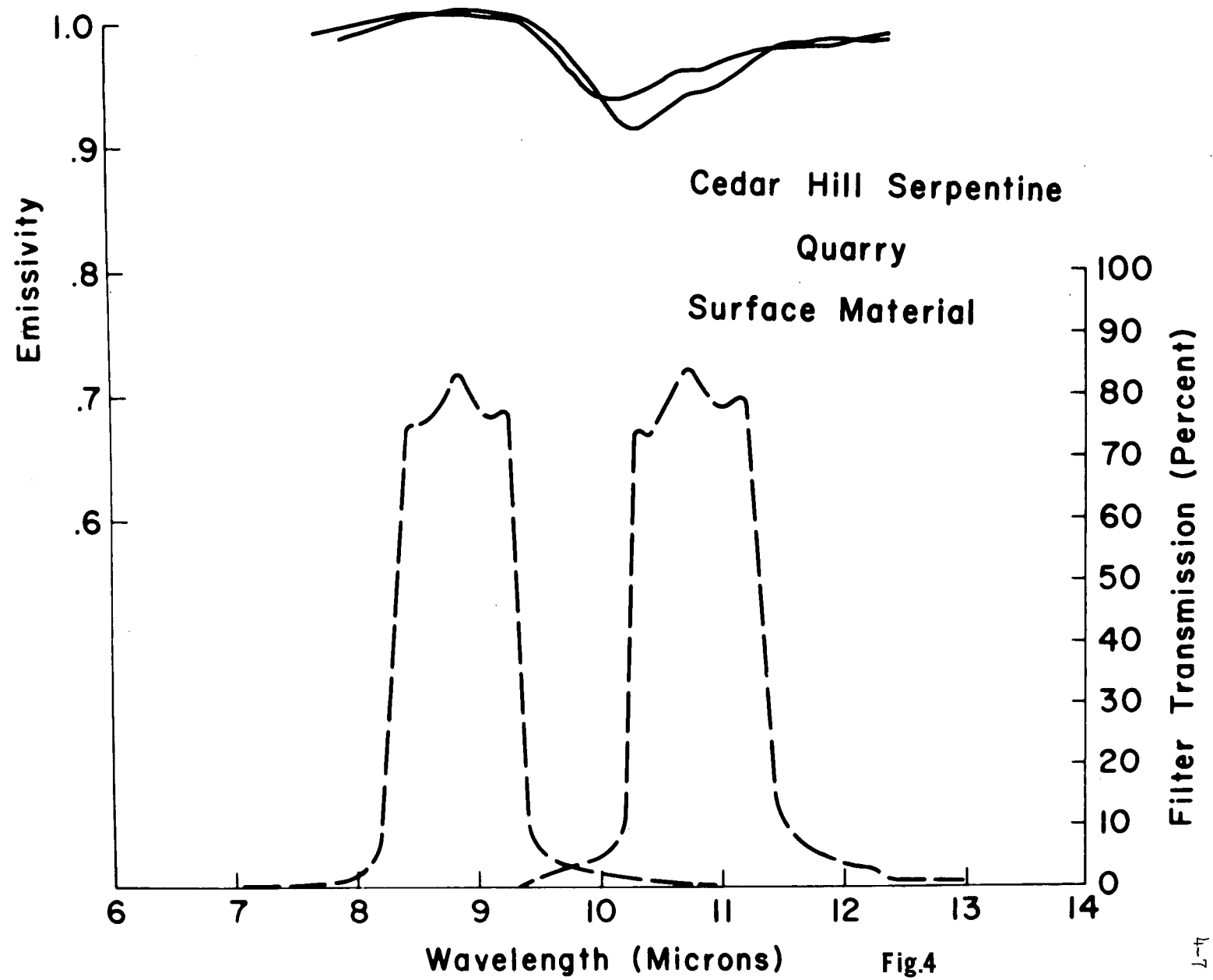


Fig.4

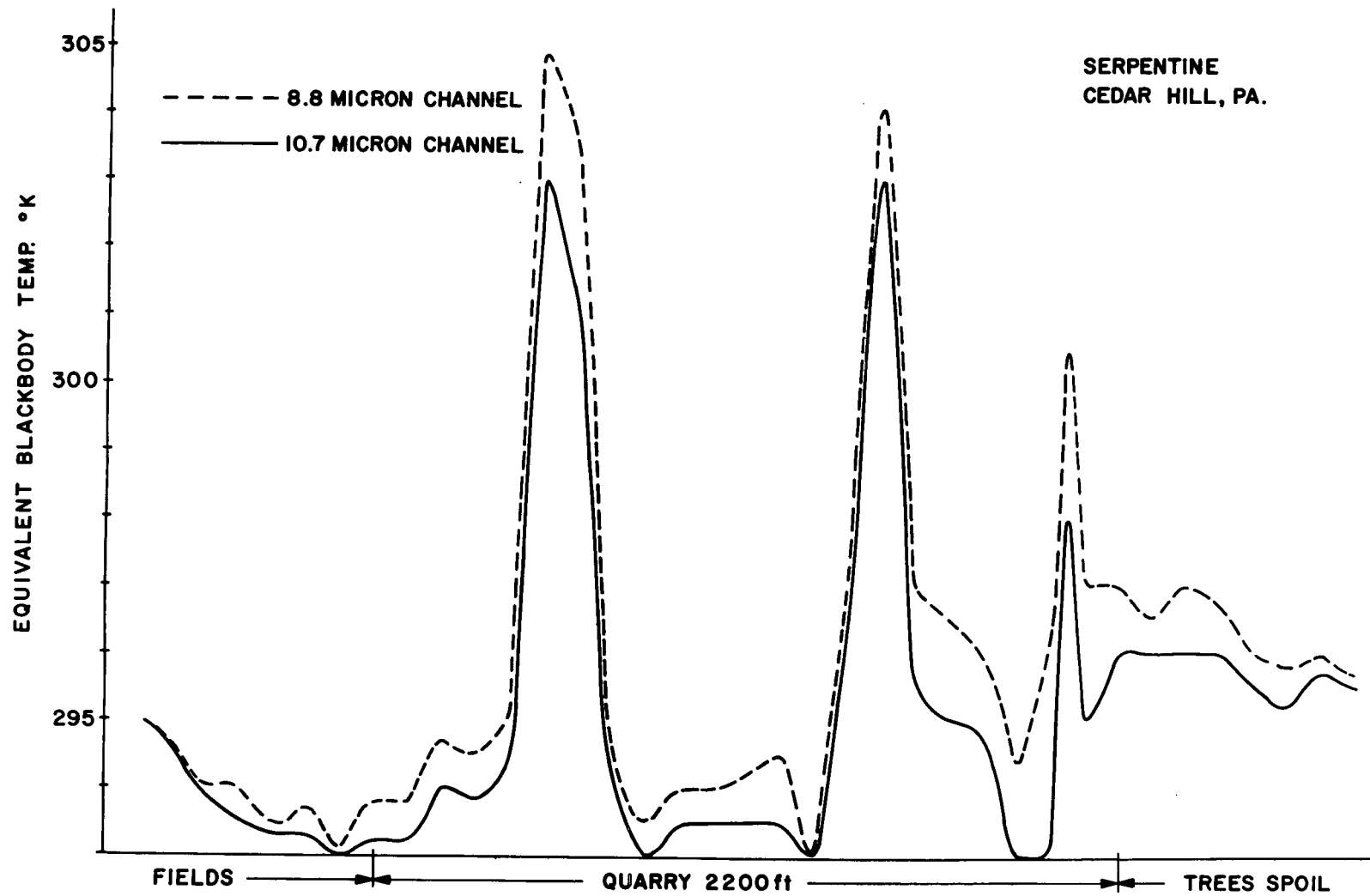


Fig.5

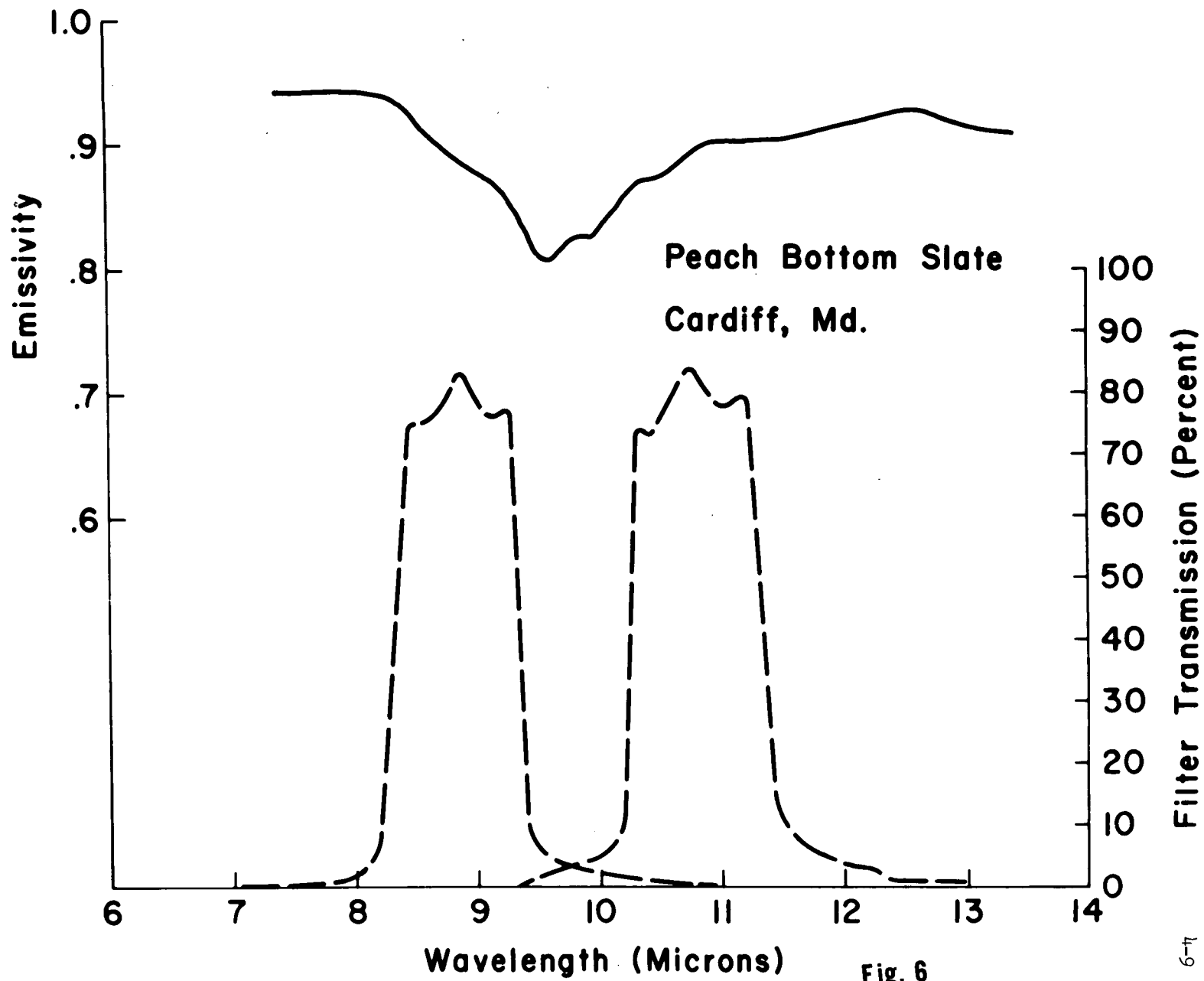


Fig. 6

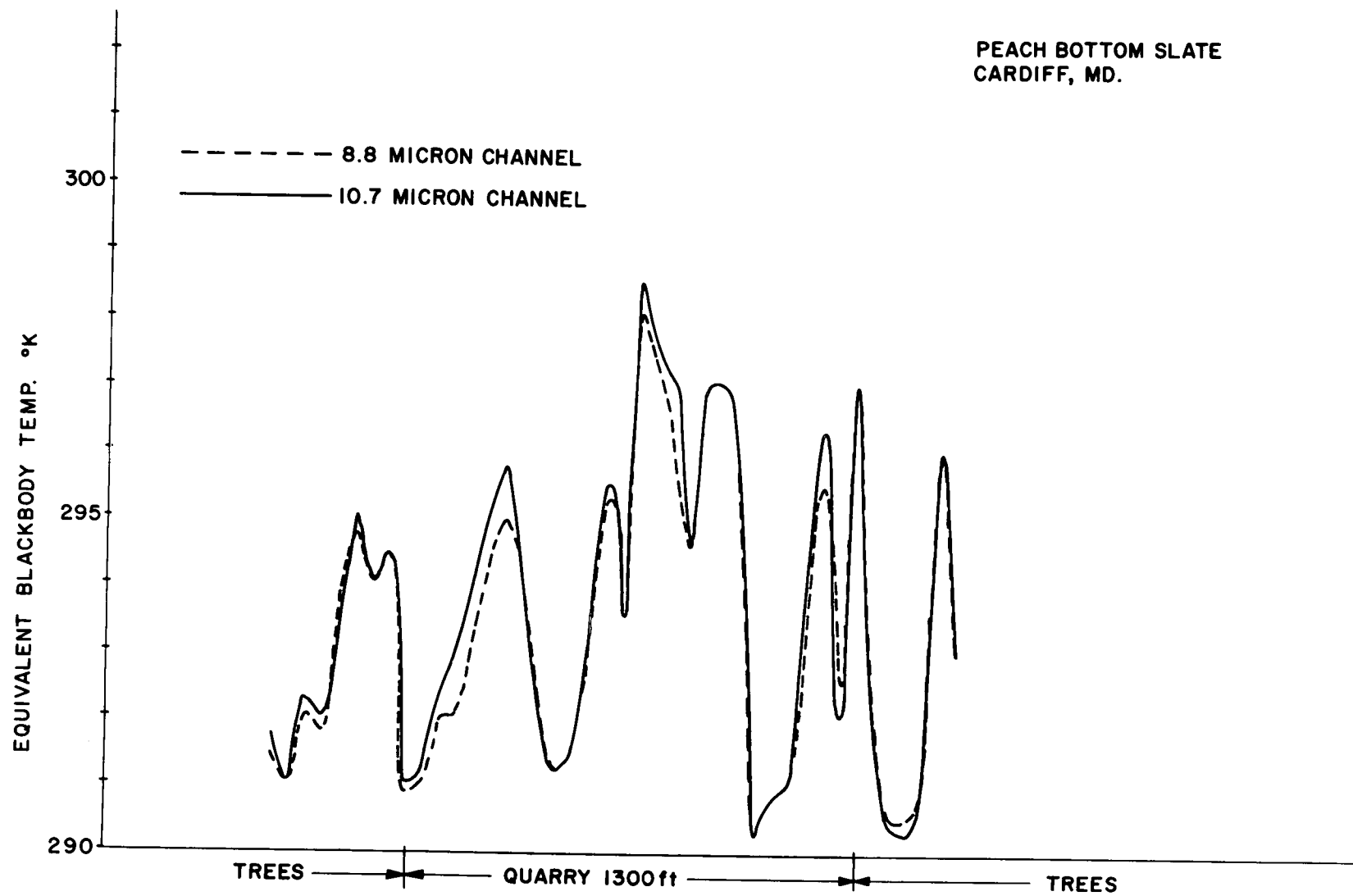


Fig. 7

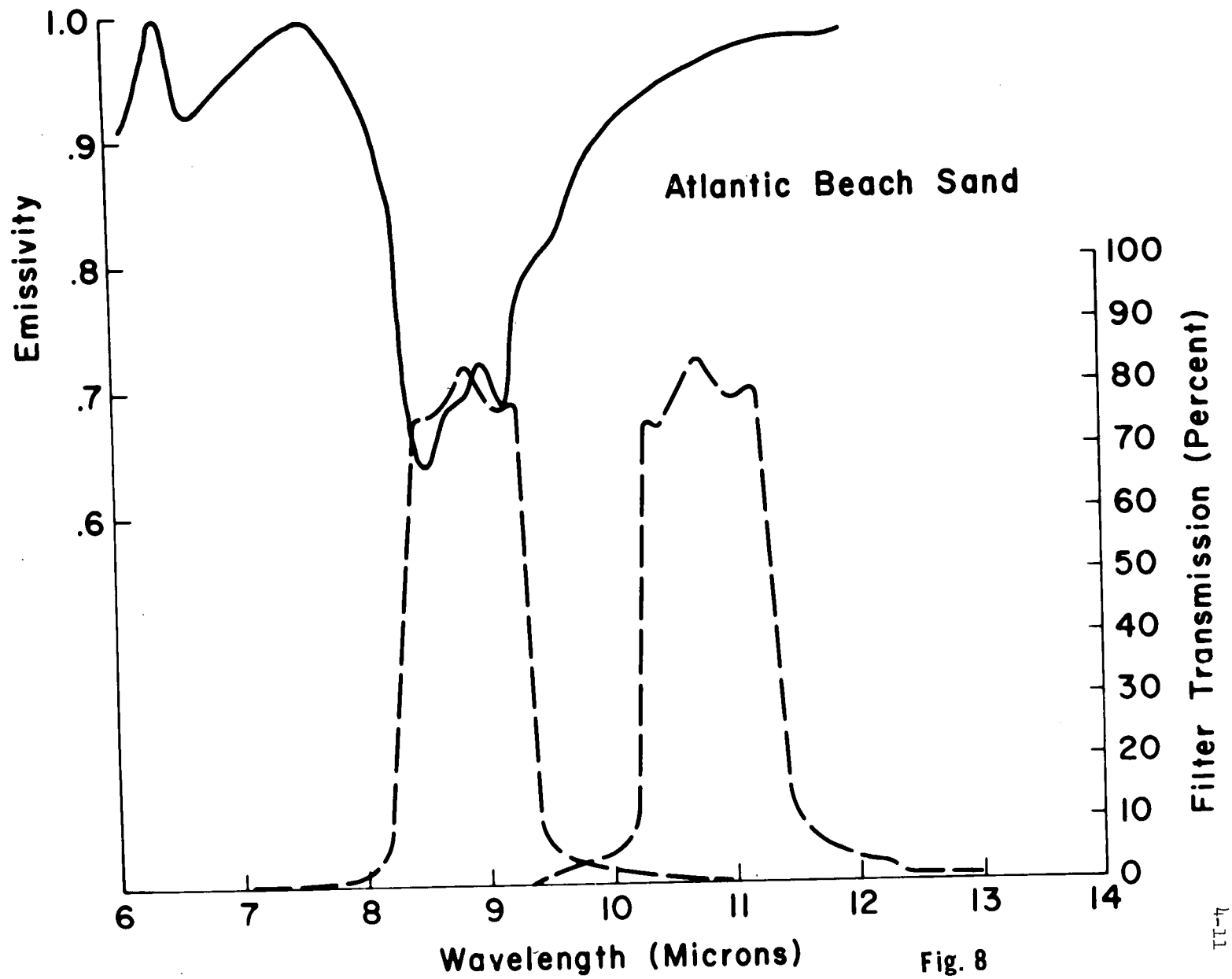


Fig. 8

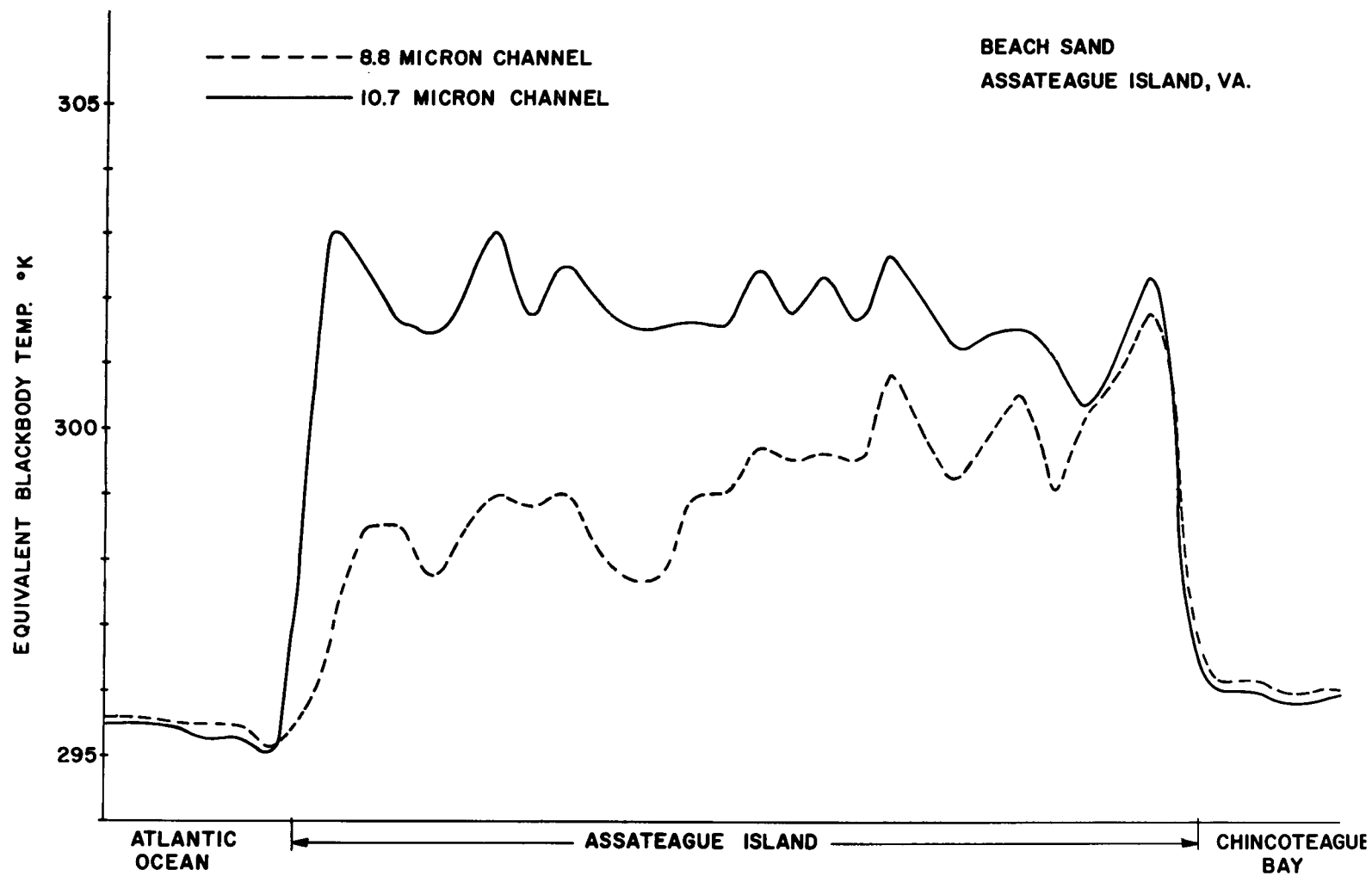


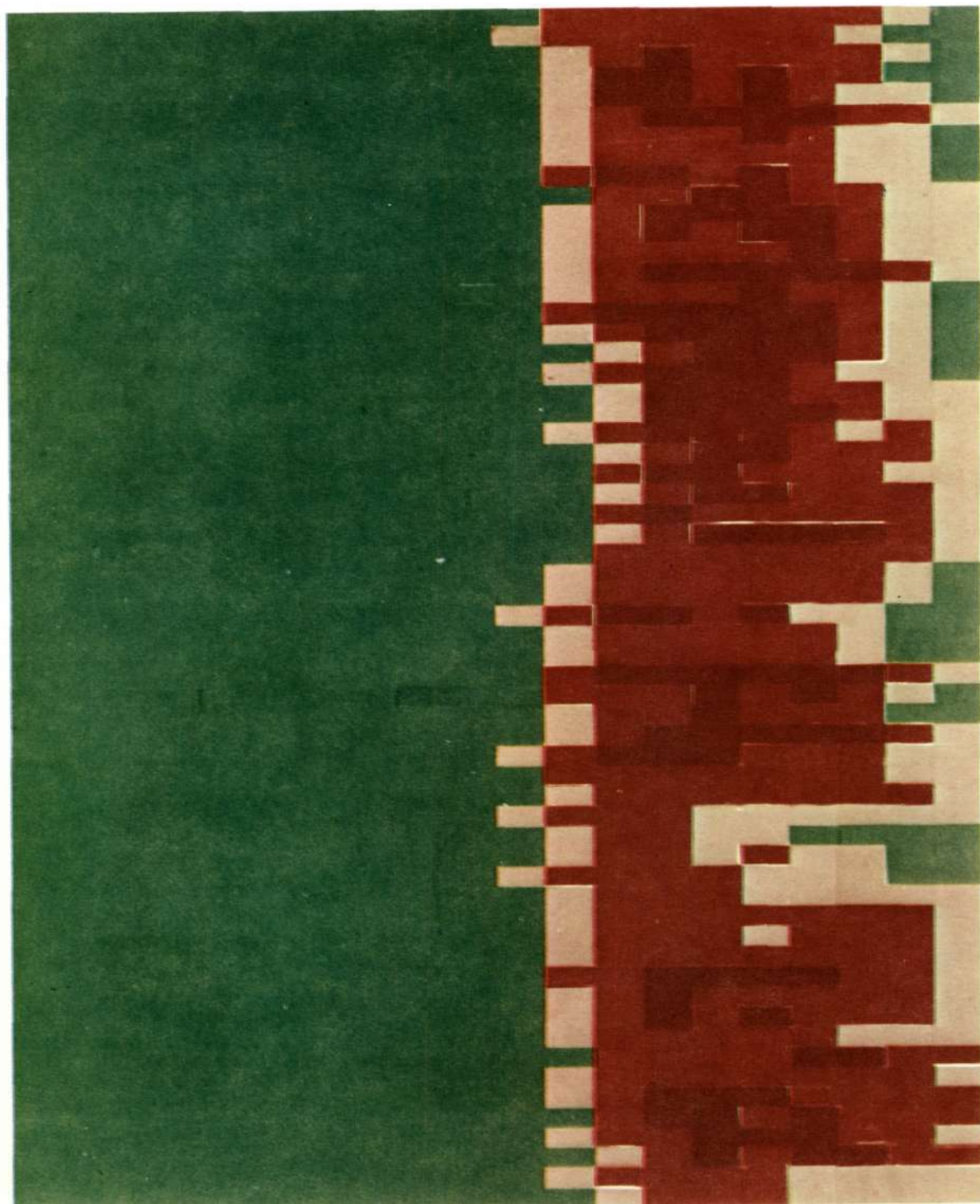
Fig. 9

—1, 0, 1

2, 3

4, 5

6, 7, 8



ASSATEAGUE ISLAND, VA.

Fig. 10